

See discussions, stats, and author profiles for this publication at: <https://www.researchgate.net/publication/272255065>

Wall current closure effects on plasma and sheath fluctuations in Hall thrusters

Article in *Physics of Plasmas* · June 2014

DOI: 10.1063/1.4885093

CITATIONS

3

READS

53

4 authors:



Winston Frias Pombo

University of Saskatchewan

14 PUBLICATIONS 69 CITATIONS

[SEE PROFILE](#)



Andrei Smolyakov

University of Saskatchewan

302 PUBLICATIONS 2,869 CITATIONS

[SEE PROFILE](#)



Igor Kaganovich

Princeton University

321 PUBLICATIONS 2,587 CITATIONS

[SEE PROFILE](#)



Y. Raitses

Princeton University

290 PUBLICATIONS 2,816 CITATIONS

[SEE PROFILE](#)

Some of the authors of this publication are also working on these related projects:



Plasma Propulsion Physics [View project](#)



PIC-MCC simulation of low-temperature plasmas [View project](#)

All content following this page was uploaded by [Y. Raitses](#) on 09 January 2016.

The user has requested enhancement of the downloaded file.

Wall current closure effects on plasma and sheath fluctuations in Hall thrusters

Winston Frias, Andrei I. Smolyakov, Igor D. Kaganovich, and Yevgeny Raitses

Citation: *Physics of Plasmas* **21**, 062113 (2014); doi: 10.1063/1.4885093

View online: <http://dx.doi.org/10.1063/1.4885093>

View Table of Contents: <http://scitation.aip.org/content/aip/journal/pop/21/6?ver=pdfcov>

Published by the [AIP Publishing](#)

Articles you may be interested in

[Effect of oscillating sheath on near-wall conductivity in Hall thrusters](#)

Phys. Plasmas **14**, 064505 (2007); 10.1063/1.2743024

[Vanishing of the negative anode sheath in a Hall thruster](#)

J. Appl. Phys. **98**, 043306 (2005); 10.1063/1.2032615

[Electron-wall interaction in Hall thrustersa\)](#)

Phys. Plasmas **12**, 057104 (2005); 10.1063/1.1891747

[Wall material effects in stationary plasma thrusters. II. Near-wall and in-wall conductivity](#)

Phys. Plasmas **10**, 4137 (2003); 10.1063/1.1611881

[Wall material effects in stationary plasma thrusters. I. Parametric studies of an SPT-100](#)

Phys. Plasmas **10**, 4123 (2003); 10.1063/1.1611880



PFEIFFER VACUUM

VACUUM SOLUTIONS FROM A SINGLE SOURCE

Pfeiffer Vacuum stands for innovative and custom vacuum solutions worldwide, technological perfection, competent advice and reliable service.

Wall current closure effects on plasma and sheath fluctuations in Hall thrusters

Winston Frias,^{1,a)} Andrei I. Smolyakov,¹ Igor D. Kaganovich,² and Yevgeny Raitses²

¹Department of Physics and Engineering Physics, University of Saskatchewan, 116 Science Place, Saskatoon, Saskatchewan S7N 5E2, Canada

²Princeton Plasma Physics Laboratory, Princeton, New Jersey 08543, USA

(Received 25 February 2014; accepted 6 June 2014; published online 26 June 2014)

The excitation of negative energy, ion sound type modes driven by the $\mathbf{E} \times \mathbf{B}$ drift and the reactive/dissipative response of the wall sheath interface is analyzed for conditions typical in a Hall thruster. Such sheath impedance modes are sensitive to the dielectric properties of the thruster wall material, which therefore may have direct influence (other than via the secondary electron emission) on fluctuations and transport. Our results predict mode frequencies consistent with the frequencies of fluctuations observed experimentally. © 2014 AIP Publishing LLC. [<http://dx.doi.org/10.1063/1.4885093>]

I. INTRODUCTION

Classical collisional transport is not large enough to explain the electron mobility observed in Hall thrusters. Two main mechanisms have been proposed for the observed anomalous transport. The first mechanism is turbulent enhancement due to the various plasma instabilities which exist in a Hall thruster.^{1–5} The exact nature of the instabilities and the specific role they play in explaining the turbulent electron transport are the subject of great interest and are currently an active area of research.^{6–15} Experimental observations suggest that wall properties also affect the electron transport.¹⁶ Electron collisions with the wall sheath have been proposed as a second mechanism responsible for the observed anomalous transport. The near wall conductivity, first proposed by Morozov,¹⁷ is sensitive to the sheath structure which in turn affects the collisions of the electrons with the wall. Both of these mechanisms, fluctuations and near wall conductivity, are thought to play a role in the conditions of the Hall thrusters.

The closure of the stationary electron current via the chamber walls has a strong influence on steady state collisional transport. This phenomenon is well documented and it is known as the Simon short circuit effect.^{19–21} The role of sheath boundary conditions on the drift wave modes was also studied in Ref. 22. Time dependent wall sheath boundary conditions (represented in terms of sheath impedance) for the dielectric wall were recently derived¹⁸ and it was shown that the fluctuations of the closure current (into the wall) may destabilize ion sound type modes in the system with $\mathbf{E}_0 \times \mathbf{B}_0$ electron drift. The sheath impedance instability strongly depends on the dielectric properties of the wall material. In the present paper, we will examine how the sheath impedance induced instability may manifest itself for the conditions typical of Hall thrusters.

II. NEGATIVE ENERGY MODES IN HALL PLASMA WITH $\mathbf{E}_0 \times \mathbf{B}_0$ ELECTRON DRIFT

The instabilities discussed in this paper are related to the ion sound modes that exist in a non-isothermal plasma such

that $T_e \gg T_i$, where T_e and T_i are the electron and ion temperature, respectively. The basic dispersion relation for such modes in a non-magnetized plasma is given by the relation $\omega^2 = k^2 c_s^2$, where $c_s = \sqrt{T_e/m_i}$ is the ion sound velocity and k is the mode wave-vector. The simplest example of the negative energy instability in Hall thruster plasma is that of the ion sound waves in the presence of the $\mathbf{E}_0 \times \mathbf{B}_0$ electron drift and electron collisions.

To fix notations consider an infinite collisionless plasma with an external magnetic field $\mathbf{B}_0 = B_0 \hat{\mathbf{z}}$ and an external electric field, perpendicular to the magnetic field, $\mathbf{E}_0 = E_0 \hat{\mathbf{x}}$. We assume finite variations along the magnetic field, $k_z \neq 0$, so that in the limit $\omega < k_z v_{Te}$, the electron inertia can be neglected ($v_{Te} = \sqrt{2T_e/m_e}$). With these assumptions, the electron equation of motion in the direction parallel to the magnetic field can be written in the form

$$0 = en_0 \nabla_{\parallel} \phi - T_e \nabla_{\parallel} \tilde{n}_e. \quad (1)$$

From this equation and assuming that the perturbed quantities vary as $e^{i(\omega t - \mathbf{k} \cdot \mathbf{r})}$, the perturbed electron density can be obtained as

$$\frac{\tilde{n}_e}{n_0} = \frac{e\phi}{T_e}. \quad (2)$$

The ion response, on the other hand, is influenced by inertia. The ion Larmor radius is assumed to be much larger than the characteristic wavelength of the perturbations and much larger than the geometric length of the system such that the ions can be considered unmagnetized. Assuming that the ions are cold, the momentum conservation and continuity equations give the ion perturbed density in the form

$$\frac{\tilde{n}_i}{n_0} = \frac{(k_y^2 + k_z^2) c_s^2 e\phi}{\omega^2 T_e}, \quad (3)$$

where k_z is the wavevector along the magnetic field, and k_y is in the azimuthal perpendicular direction. Thus, the dispersion relation for the (stable) ion sound waves in Hall plasmas is obtained from the quasineutrality condition and Eqs. (2) and (3)

^{a)}Electronic mail: wpf274@mail.usask.ca.

$$\omega^2 = (k_y^2 + k_z^2)c_s^2. \quad (4)$$

It is worth noting here that the equilibrium electron velocity $\mathbf{v}_0 = c\mathbf{E}_0 \times \mathbf{B}_0/B_0^2$ does not enter the above dispersion relation. In fact, the effect of the Doppler shift due to the electron flow \mathbf{v}_0 is hidden in the response of the parallel electron current. Though this current is not explicitly present in Eqs. (1)–(3), it is finite. It can be found from the electron continuity equation

$$\frac{\partial \tilde{n}_e}{\partial t} + v_0 \cdot \nabla \tilde{n}_e + n_0 \frac{\partial \tilde{v}_{ez}}{\partial z} = 0, \quad (5)$$

which gives

$$\tilde{J}_{e\parallel} = -e(\omega - \omega_0)\tilde{n}_e/k_z, \quad (6)$$

where $\omega_0 = \mathbf{k} \cdot \mathbf{v}_0$ is the drift frequency.

It is seen from Eq. (6) that the parallel electron current is affected by the magnetic field and exhibits a Doppler shift with respect to the density perturbations. In an infinite plasma, the parallel (along the magnetic field) electron current remains arbitrary but finite. A coupling between the parallel electron current and the density and potential perturbations would modify the wave dynamics. The simplest feedback mechanism that can produce this coupling is provided by electron collisions. The electron equation of motion, Eq. (1), including collisions can be written as

$$\begin{aligned} e n_0 \nabla_{\parallel} \phi - T_e \nabla_{\parallel} \tilde{n}_e - m_e n_0 \nu_e \tilde{v}_{ez} &= 0, \\ i k_z \left(\phi - \frac{T_e \tilde{n}_e}{e n_0} \right) + \frac{m_e \nu_e}{e^2 n_0} \tilde{J}_{e\parallel} &= 0, \end{aligned} \quad (7)$$

where ν_e is the electron collision frequency. The perturbed electron density can now be written from Eq. (7) as

$$\frac{\tilde{n}_e}{n_0} = \frac{e\phi}{T_e} \frac{1}{1 - i\nu_e(\omega - \omega_0)/k_z^2 v_{Te}^2/2}. \quad (8)$$

Combining the ion and electron density perturbations from Eqs. (3) and (8) and using quasineutrality, the following dispersion relation is obtained:

$$\omega = k c_s \left(1 - i \frac{\nu_e(\omega - \omega_0)}{2k_z^2 v_{Te}^2} \right). \quad (9)$$

The dispersion relation in Eq. (9) describes ion sound waves destabilized by electron collisions.¹⁸ The condition $\omega < \omega_0$ is required for the growth rate of the instability to be positive. The equilibrium electron flow \mathbf{v}_0 is a source of free energy for this instability. Normally, perturbations from the full thermodynamic equilibrium, have positive energy, e.g., the kinetic energy is such that $E = \int mv^2/2 d\tau > 0$, where $d\tau$ is the respective volume element, and v is the perturbed velocity. In systems thermodynamically away from equilibrium, such as in a system with a finite flow in the equilibrium state, the perturbations which have a phase velocity lower than the equilibrium velocity, $v_{ph} < \mathbf{v}_0$, may have a total energy in the perturbed state lower than the equilibrium energy related to the stationary flow, \mathbf{v}_0 : $E' = \int mv^2 d\tau/2 < E_0 = \int mv_0^2 d\tau/2$; here $v = v_0 + v'$ is the total velocity, which includes an

equilibrium part v_0 and a perturbation v' . These are the so called negative energy perturbations,²³ see also Ref. 24 and references therein. The amplitude of such perturbations increases when the energy is removed from the system, e.g., turning into heat due to dissipation. This way, dissipation may destabilize the negative energy mode. Alternatively, the coupling of two modes, one with negative and other with positive energy, may lead to a reactive instability where both modes would grow via energy transfer from the negative energy mode to the mode with positive energy.

In the ion sound instability example considered above, the dissipation is due to the electron collisions, which remove energy from the fluctuations. The coupling of the perturbed electron current, density and potential fluctuations creates the phase shift between current and potential which produces the instability via a positive feedback mechanism that feeds the initial perturbations.

III. SHEATH BOUNDARY CONDITIONS AND SHEATH INDUCED INSTABILITIES

Another feedback mechanism in a finite length plasma, and the focal one for this paper, arises when the sheath boundary conditions are included. The sheath boundary conditions determine the electron current to the walls resulting in coupling of perturbed plasma density and potential to produce the instabilities in a process similar to that described in the example in Sec. II. Consider a plasma between two walls separated by a distance of $2H$, where the equilibrium magnetic field $\mathbf{B}_0 = B_0 \hat{\mathbf{z}}$ is in the radial direction normal to the walls, the equilibrium electric field $\mathbf{E}_0 = E_0 \hat{\mathbf{x}}$ is in the axial direction and the electrons drift along the azimuthal y direction with a velocity $\mathbf{v}_0 = c\mathbf{E}_0 \times \mathbf{B}_0/B_0^2$ as in a Hall thruster (see Fig. 1). In stationary state, the ion current to the sheath is equal to the Bohm current

$$J_{i0} = en_0 c_s, \quad (10)$$

while the electron current is determined by the electrons in the tail of the (Maxwellian) distribution function with energies above the potential drop in the sheath $\phi_0 = \phi_p - \phi_w$,

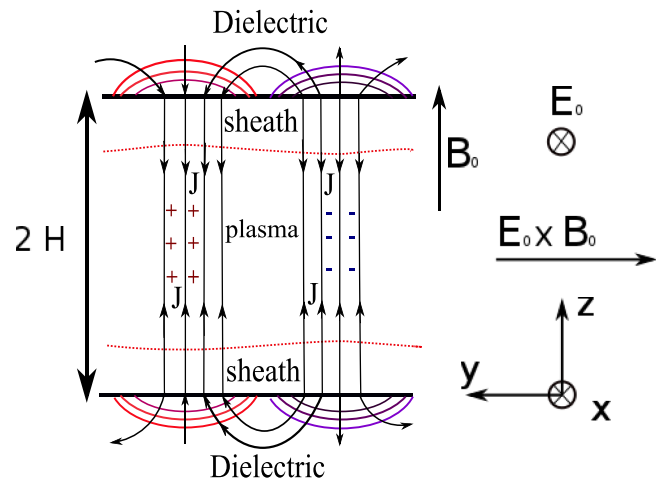


FIG. 1. The instability is driven by the component of the perturbed parallel current that is directed into the regions of positive charge (shown with “+”), thus enhancing the initial perturbation.

where ϕ_p is the plasma potential at the plasma-sheath edge and ϕ_w is the wall potential

$$J_{0e} = -\frac{en_0v_{Te}}{2\sqrt{\pi}} \exp\left(-\frac{e(\phi_p - \phi_w)}{T_e}\right). \quad (11)$$

In stationary state, the total current into the sheath is zero, e.g., $J_{0e} + J_{0i} = 0$. The perturbed ion and electron currents are determined by the density, potential, and temperature perturbations given by Eqs. (10) and (11) as

$$\tilde{J}_i = \left(\frac{\tilde{n}_i}{n_0} + \frac{1}{2} \frac{\tilde{T}_e}{T_{e0}}\right) J_{0i}, \quad (12)$$

$$\tilde{J}_e = \left[\frac{\tilde{n}_e}{n_0} + \frac{1}{2} \frac{\tilde{T}_e}{T_{e0}} - \left(\frac{e(\tilde{\phi}_p - \tilde{\phi}_w)}{T_e} - \Lambda \frac{\tilde{T}_e}{T_{e0}}\right)\right] J_{0e}, \quad (13)$$

where $\Lambda = \ln\sqrt{m_i/2\pi m_e}$. The parallel current to the sheath is the sum of the ion and electron currents from Eqs. (12) and (13). The total sheath current can then be expressed, neglecting temperature fluctuations, as¹⁸

$$\tilde{J}_{sh} = \frac{e^2 n_0 c_s}{T_e} (\tilde{\phi}_p - \tilde{\phi}_w). \quad (14)$$

If we have a conductive wall, $\tilde{\phi}_w = 0$, the sheath current results in dissipation, the so called sheath resistivity.^{25–28} In the case of a dielectric wall, one can assume that due to current conservation, the current at the plasma sheath edge is equal to the displacement current in the dielectric wall. Using the potential at the wall as a boundary condition and assuming that $k_z H \gg 1$, where H is the half width of the channel, the potential at the wall can be written as function of the potential in the wall plasma¹⁸

$$\tilde{\phi}_w = \tilde{\phi}_p \frac{1}{1 - i\varepsilon\omega|k_y|c_s/\omega_{pi}^2}, \quad (15)$$

where ε is the dielectric constant of the wall material and ω_{pi} is the ion plasma frequency. Using Eqs. (14) and (15), the current into the sheath can be written as a function of the perturbations of the plasma potential as

$$\tilde{J}_{sh} = -\frac{e^2 n_0 c_s}{T_e} \tilde{\phi}_p \frac{iK}{1 - iK}, \quad (16)$$

where $K \equiv \varepsilon\omega|k_y|c_s/\omega_{pi}^2$. The value of the K parameter depends on the mode wave-vector k_y and the dielectric constant ε .

The expression for the sheath current that couples the perturbed plasma density, potential and current can be used to derive the dispersion relation for two types of modes. One of these modes is characterized by long wavelengths such that $H\partial/\partial z \ll 1$, while the other modes take into account the variations along the magnetic field. In both cases, the modes are rendered unstable due to the parallel component of the current that is directed into the regions of positive charge and enhances the initial perturbations, as illustrated in Fig. 1.

To study the long wavelength global modes, consider a long plasma tube between the walls $z = -H$ and $z = H$ (see Fig. 1). The electron and ion continuity equations, neglecting variations along the axial direction, can be written as

$$\frac{\partial \tilde{n}_e}{\partial t} + v_0 \frac{\partial \tilde{n}_e}{\partial y} - \frac{1}{e} \frac{\partial \tilde{J}_{\parallel e}}{\partial z} = 0, \quad (17)$$

$$\frac{\partial \tilde{n}_i}{\partial t} - i \frac{en_0}{m_i \omega} \frac{\partial^2 \tilde{\phi}}{\partial y^2} + \frac{1}{e} \frac{\partial \tilde{J}_{\parallel i}}{\partial z} = 0. \quad (18)$$

We can introduce the average density and potential as

$$\bar{n} \equiv \frac{1}{2H} \int_{-H}^H \tilde{n} dz, \quad (19)$$

$$\bar{\phi} \equiv \frac{1}{2H} \int_{-H}^H \tilde{\phi} dz, \quad (20)$$

and the ion and electron continuity equations can be averaged, assuming an odd parity for the parallel currents ($J_{\parallel}(-H) = -J_{\parallel}(H)$), to produce

$$-i(\omega - \omega_0)\bar{n} - \frac{J_{\parallel e}(H)}{eH} = 0, \quad (21)$$

$$-i\omega\bar{n} + ien_0 \frac{k_y^2 \bar{\phi}}{\omega m_i} + \frac{J_{\parallel i}(H)}{eH} = 0, \quad (22)$$

where $J_{\parallel e}(H)$ and $J_{\parallel i}(H)$ are the electron and ion currents at the sheath boundary, given by Eqs. (12) and (13),

$$J_{\parallel i}(H) = \frac{n(H)}{n_0} J_{0i}, \quad (23)$$

$$J_{\parallel e}(H) = \frac{n(H)}{n_0} J_{0e} + \frac{iK}{1 - iK} \frac{e}{T_e} \phi(H) J_{0e}. \quad (24)$$

From Eqs. (19)–(24), it can be seen that the electron current exhibits a Doppler shift while the ion current does not. Introducing the sheath collision frequency, $\nu_{sh} = c_s/H$, and using the expressions obtained for the currents above, the perturbed average ion and electron densities are given by¹⁸

$$\frac{\bar{n}_i}{n_0} = \frac{k_y^2 c_s^2}{\omega(\omega + i\nu_{sh})} \frac{e\bar{\phi}}{T_e}, \quad (25)$$

$$\frac{\bar{n}_e}{n_0} = \frac{\nu_{sh} K}{(1 - iK)(\omega - \omega_0 + i\nu_{sh})} \frac{e\bar{\phi}}{T_e}. \quad (26)$$

Using quasineutrality and assuming that $K < 1$ (dielectric), we can obtain the following dispersion relation:¹⁸

$$\omega^2(\omega + i\nu_{sh}) = \frac{|k_y|c_s\omega_{pi}^2}{\varepsilon\nu_{sh}} (\omega - \omega_0 + i\nu_{sh}). \quad (27)$$

The mode described by Eq. (27) has an unstable root for $\omega < \omega_0$, given by

$$\omega_r \simeq \gamma \simeq \left(-\frac{\omega_0 |k_y| c_s \omega_{pi}^2}{\varepsilon \nu_{sh}} \right)^{1/3}, \quad (28)$$

which corresponds to a reactive instability of the negative energy mode similar to the one described at the beginning of this section. In the opposite limit, $K \gg 1$, the instability becomes dissipative with a real part of the frequency and a growth rate of

$$-\omega_r \simeq \gamma \simeq \left(\frac{|\omega_0| k_y^2 c_s^2}{2\nu_{sh}} \right)^{1/2}. \quad (29)$$

The transition between the two limits, $K < 1$ and $K > 1$, is controlled by the mode frequency and the value of the dielectric constant ε . The limit of an infinitely conducting wall can be obtained formally by taking $\varepsilon \rightarrow \infty$.

The effect of the ion convection is manifest in the inclusion of the term $k_x V_{0i}$, where k_x is the wavevector in the axial direction and $V_{0i} = \sqrt{2e\phi/m_i}$ is the equilibrium ion velocity due to the electric field. When this term is included, the dispersion relation for the long wavelength (global) modes given by Eq. (27) becomes

$$\omega(\omega - k_x V_{0i})(\omega - k_x V_{0i} + i\nu_{sh}) = \frac{|k_y| c_s \omega_{pi}^2}{\varepsilon \nu_{sh}} (\omega - \omega_0 + i\nu_{sh}). \quad (30)$$

Considering that the Hall thruster channel length, L_x , is of the order of 0.1 m, the axial wavevector is $k_x = 2\pi/L_x \approx 62.83$ rad/m and the maximum ion equilibrium velocity is of the order of 10^4 m/s, the ion convection frequency for the long wavelength modes is $f_i = k_x V_{0i}/2\pi \approx 10^5$ Hz, which is lower than the typical frequencies of the global and local modes obtained in this paper.

The local modes are obtained when the variations along the magnetic field are taken into account. The eigenmodes obtained in this case depend on both the z (parallel to the magnetic field) and y (perpendicular to the magnetic field) coordinates. In general, these perturbations can be expressed as the sum of a mode with both z and y dependence and a boundary mode that depends only on y

$$\phi = [\phi_0 \cos(k_z z) + \phi_b] e^{i(k_y y - \omega t)}, \quad (31)$$

$$n = \frac{en_0}{T_e} \left[\phi_0 \cos(k_z z) + \phi_b \frac{k_y^2 c_s^2}{\omega^2} \right] e^{i(k_y y - \omega t)}. \quad (32)$$

Here, ω is given by Eq. (4), k_y is a free parameter determined from the geometry and boundary conditions of the region of interest and k_z is an eigenvalue that is calculated from the solvability condition of the linear system obtained from the ion and electron continuity and momentum conservation equations.

Coupling to the sheath follows from the averaged electron and ion equations (21) and (22), where now the average potential and density over the region from $z = -H$ to $z = H$ can be calculated using Eqs. (31) and (32) to produce

$$\bar{\phi} = \left[\phi_0 \frac{\sin(k_z H)}{k_z H} + \phi_b \right] \exp(-i\omega t + ik_y y), \quad (33)$$

$$\bar{n} = \frac{en_0}{T_e} \left[\phi_0 \frac{\sin(k_z H)}{k_z H} + \phi_b \frac{k_y^2 c_s^2}{\omega^2} \right] \exp(-i\omega t + ik_y y). \quad (34)$$

Replacing the values for the currents in Eqs. (23) and (24) and the averaged density and potential from Eqs. (33) and (34) in the electron continuity equation (21), one obtains

$$\begin{aligned} & \phi_b \left(-i(\omega - \omega_0) \frac{k_y^2 c_s^2}{\omega^2} + \nu_{sh} \frac{k_y^2 c_s^2}{\omega^2} + \nu_{sh} \frac{iK}{1 - iK} \right) \\ & + \phi_0 \left(-i(\omega - \omega_0) \frac{\sin k_z H}{k_z H} + \frac{\nu_{sh} \cos k_z H}{1 - iK} \right) = 0. \end{aligned} \quad (35)$$

Using quasineutrality, the ion continuity equation (22) can be written as

$$i\omega_0 \bar{n} + i \frac{en_0}{\omega m_i} k_y^2 \bar{\phi} + \frac{1}{eH} \frac{iK}{1 - iK} \frac{e}{T_e} \phi(H) J_{0e} = 0,$$

or

$$\begin{aligned} & \phi_0 \left(i\omega_0 \frac{\sin k_z H}{k_z H} - i \frac{k_y^2 c_s^2}{\omega} \frac{\sin k_z H}{k_z H} + \frac{iK \nu_{sh} \cos k_z H}{1 - iK} \right) \\ & + \phi_b \left(-i(\omega - \omega_0) \frac{k_y^2 c_s^2}{\omega^2} + \nu_{sh} \frac{iK}{1 - iK} \right) = 0. \end{aligned} \quad (36)$$

From Eqs. (35) and (36), a 2×2 linear system for ϕ_b and $\phi_0 \cos(k_z H)$ is obtained. The solvability condition for this system of equations yields the dispersion relation for the small scale (local) modes as¹⁸

$$\begin{aligned} & \frac{\tan(k_z H)}{k_z H} \times \left[\omega_0 - \frac{k_y^2 c_s^2}{\omega} - \frac{i\omega(\omega - \omega_0)}{\nu_{sh}} \left(1 - \frac{k_y^2 c_s^2}{\omega^2} \right) \right. \\ & \left. + i\omega \left(\frac{\omega^2}{k_y^2 c_s^2} - 1 \right) \frac{K}{1 - iK} \right] \\ & + \left[\omega - \omega_0 + \frac{\nu_{sh}}{1 - iK} - \nu_{sh} \frac{\omega^2}{k_y^2 c_s^2} \frac{K}{1 - iK} \right] = 0. \end{aligned} \quad (37)$$

The eigenvalues for ω can be obtained by solving Eq. (37) together with the dispersion relation in Eq. (4). The local and global modes dispersion relation have been studied in detail in Ref. 18. The dispersion relations predict perturbations which have azimuthal phase velocity in the direction of the electron $\mathbf{E}_0 \times \mathbf{B}_0$ drift. The growth rate and absolute value of the frequency of the unstable modes grow with the height of the channel, and the electron drift velocity ω_0 . The growth rate also exhibits a $1/\sqrt{m_i}$ dependence. The absolute value of the real part of the frequency and the growth rate tend to decrease with increasing dielectric permittivity, but they do not completely disappear in the limit $\varepsilon \rightarrow \infty$ which would correspond to the case of the fully conducting wall with $\phi_w = 0$.

IV. SHEATH INDUCED MODES IN HALL THRUSTER

The instabilities studied in Sec. III can be thought of as resulting from a positive feedback mechanism between the Doppler shifted parallel electron current and fluctuations of plasma density and potential. In this section, we investigate characteristic frequencies for these instabilities in conditions typical for the Hall thruster. As an example, we will use generic parameters from the 1 kW Laboratory Hall thruster developed at the PPPL Hall Thruster Experimental facility.^{29,31} This thruster has a channel made of boron nitride ceramic (BN) and has length of 90 mm (from anode to channel exit) and a mean radius of 36 mm.³¹ For our study, we will use measured plasma parameters for the acceleration and exit region of the thruster as reported in Ref. 29.

The growth rate and frequency obtained from Eqs. (27) and (37) using the plasma parameters corresponding to the 1 kW Laboratory Hall thruster are shown in Fig. 2. The instabilities are present in the region that extends from 8 mm upstream from the channel exit to the exit of the channel.

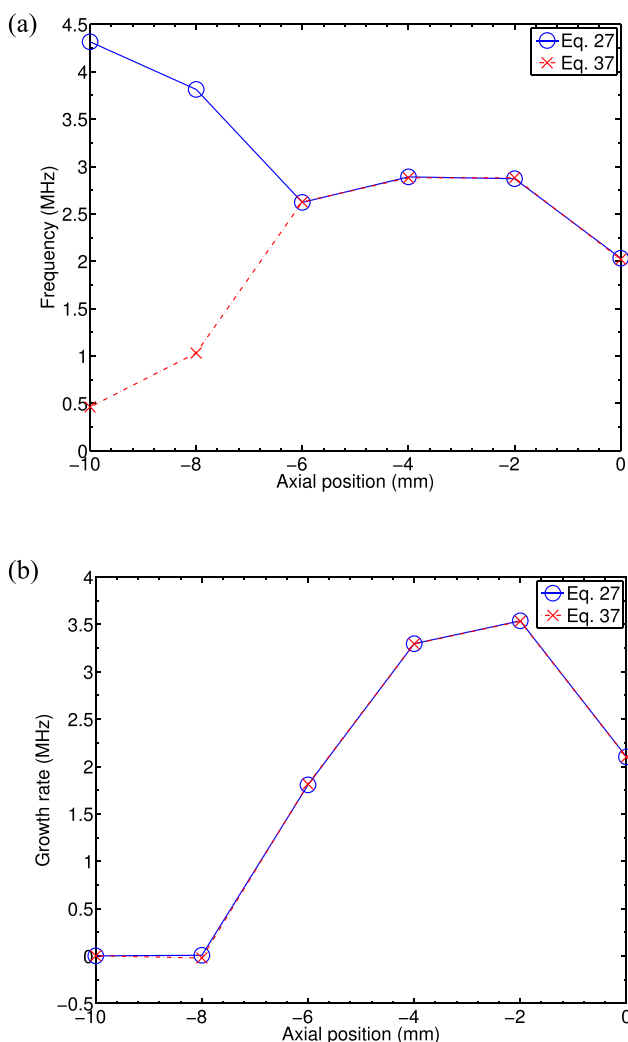


FIG. 2. Frequency and growth rate of the instabilities in the 1 kW Laboratory Hall thruster²⁹ as a function of axial position from the channel exit as predicted by Eqs. (27) and (37); $k_y = 28$ rad/m ($m = 1$). The anode is located at $x = -36$ mm. The exit plane is at $x = 0$.

The growth rate and the real part of the frequency of the instabilities predicted by the global modes in Eq. (27) reach maximum values of $f = 2.88$ MHz and $\gamma = 3.53$ MHz 2 mm upstream from the channel exit. The real part of the frequency and the growth rate of the instabilities predicted by the local modes in Eq. (37) reach maximum values of $f = 2.88$ MHz and $\gamma = 3.53$ MHz, also 2 mm upstream from the exit of the thruster channel. It turns out that for these parameters, the growth rate and frequency for the global and local modes are identical. These calculated frequencies are of the same order of magnitude as the azimuthal modes experimentally observed by Litvak *et al.*²⁹ The calculated azimuthal phase velocity of the instabilities for the lowest azimuthal mode number ($m = 1$) is shown in Fig. 3. The azimuthal phase velocity for the global modes reaches a maximum value of 6.52×10^5 m/s at 2 mm upstream from the channel exit. The maximum value for the azimuthal phase velocity of the local modes is reached at 2 mm upstream from the channel exit and has a value of 6.52×10^5 m/s. The equilibrium $E_0 \times B_0$ electron drift velocity has a maximum value of 2.25×10^6 m/s also at 2 mm upstream from the channel exit. Thus, the phase velocities of both local and global modes are below the equilibrium electron drift velocity, meaning that the instability is of the negative energy type. The phase velocity of the unstable modes reported by Litvak *et al.* has a maximum value of the order of 1.75×10^6 m/s also at 2 mm upstream from the channel exit. The instability reported in the current paper is also characterized by having a real part of the frequency that decreases with increasing magnetic field and increases with increasing electric field as can be seen in Fig. 4. These results agree with the results obtained by Litvak *et al.* (compare with Fig. 7 from Ref. 29).

Another device of interest is the SPT-100 Hall thruster. The SPT-100 thruster has dielectric walls made of Borosil (BNSiO_2) whose dielectric constant, ϵ , is 3.50–3.75. The

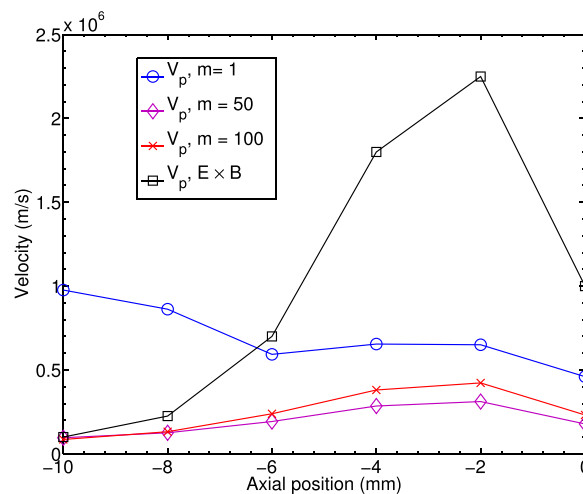


FIG. 3. Azimuthal phase velocities of the instabilities in the 1 kW Laboratory Hall thruster²⁹ as a function of axial position as predicted by Eqs. (27) and (37) for different mode numbers and the equilibrium $E_0 \times B_0$ electron drift velocity, $k_y = m/r$, $r = 3.6$ cm. The anode is located at $x = -36$ mm. The exit plane is at $x = 0$.

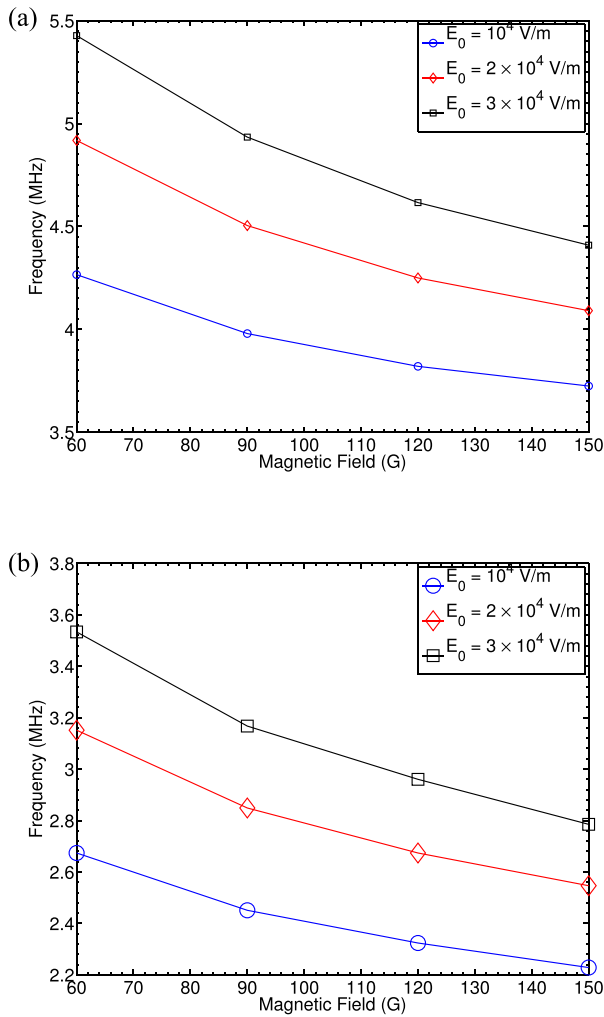


FIG. 4. Frequency of the modes predicted by Eqs. (27) (a) and (37) (b) as a function of the magnetic field for different values of the electric field in 1 kW Laboratory Hall thruster,²⁹ $k_y = 28$ rad/m ($m = 1$).

channel width is 1.50 cm and the mid radius of the thruster is 5 cm.³⁰ The growth rates and frequency obtained from Eqs. (27) and (37) using the plasma parameters in the discharge chamber of SPT-100 Hall thruster obtained by Hoffer with the HPHall-2 code^{32,33} as reported in Ref. 30 are shown in Fig. 5. For these conditions, the instabilities are present in the region located 9 mm upstream from the channel exit for the local modes. The global modes predict instability for the channel region, but the growth rate is small reaching a value of 1 MHz at around 8 mm upstream from the channel exit and a maximum value of 3.03 MHz 2 mm upstream from the exit plane. The real part of the frequency of the instabilities predicted by the global modes Eq. (27) reaches a value of 2.554 MHz at the exit of the channel, while the frequency for the local modes reaches a value of 2.5 MHz at the channel exit. These values correspond to azimuthal phase velocities at the exit plane of 8.03×10^5 m/s for the both the global and local modes. Similarly to the case with the 1 kW Laboratory Hall Thruster, the real part of the frequency and the growth rates for the local and global modes are very close.

The results obtained for the SPT-100 parameters are similar to high frequency instabilities reported by

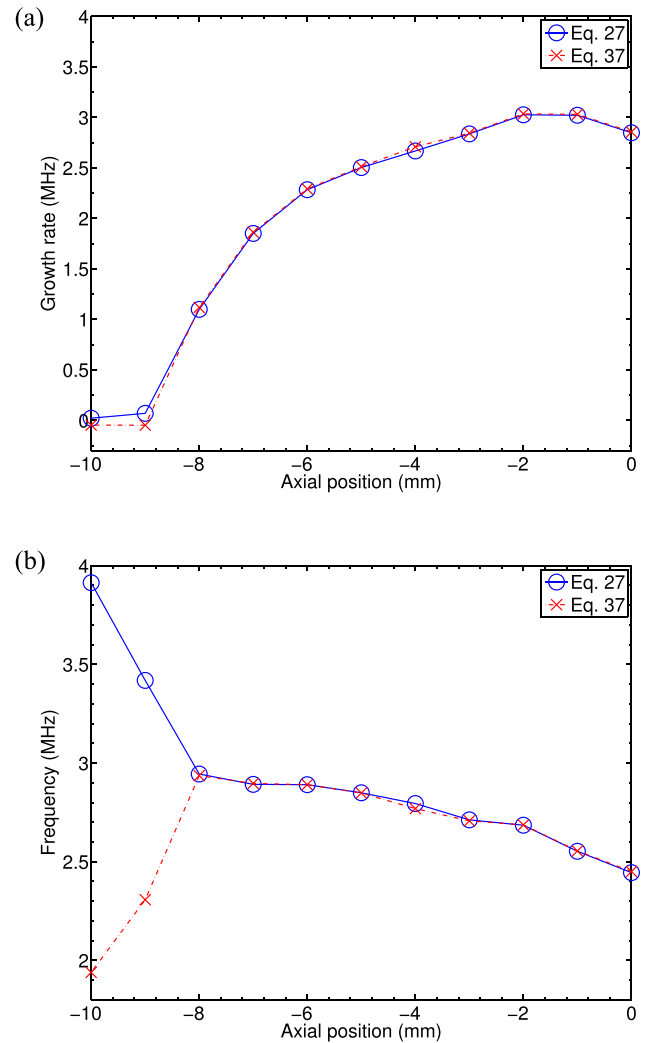


FIG. 5. Frequency and growth rate of the instabilities in a SPT-100 thruster³⁰ as a function of axial position from the channel exit as predicted by Eqs. (27) and (37), $k_y = 20$ rad/m ($m = 1$, poloidal mode number). The exit plane is at $x = 0$.

Lazurenko *et al.*¹³ Lazurenko *et al.* studied high frequency instabilities in the 1.5 kW SPT-100ML and 5 kW PPS-X000ML Hall thrusters. They observed a high frequency mode in the region directly downstream from the peak of the magnetic field inside the channel and in the near exit region that propagates azimuthally with a phase velocity of 2.0×10^6 m/s, which corresponds to a frequency of 7–9 MHz for the lowest azimuthal mode.¹³ This velocity is close to the expected electron equilibrium $E_0 \times B_0$ velocity. The real part of the frequency of the instabilities reported by Lazurenko *et al.* increases with increasing discharge voltage (see Fig. 10 in Ref. 13). Also, a decrease of the frequency with increasing magnetic field in the PPS-X000ML Hall thruster is reported.¹³ This is similar to the trend observed in the experiments from Ref. 29.

As noted above, in the channel exit region, the real part of the frequency and the growth rate of the instabilities predicted by both global and local dispersion relations are identical. The frequency of the local modes, ω , and eigen-value wavenumber in the direction parallel to the magnetic field, k_z , are calculated using Eqs. (4) and (37). For the frequencies

predicted by the local modes in the channel exit region, the obtained parallel (to the magnetic field) wavenumber are such that the factor $\tan(k_z H)/k_z H$ is small, $\tan(k_z H)/k_z H \ll 1$. Taking this into account, the equation for the local modes in the region close to the channel exit can be written as

$$k_y^2 c_s^2 (\omega - \omega_0) = \omega^2 \frac{\nu_{sh} K}{1 - iK}. \quad (38)$$

In the exit region, we have $K \ll 1$ and the sheath collision frequency ν_{sh} smaller than both the frequency of the instability and the electron drift frequency. This allows us to write the equation for the local modes in this region as

$$\omega^3 = \frac{|k_y| c_s \omega_{pi}^2}{\epsilon \nu_{sh}} (\omega - \omega_0), \quad (39)$$

which is the same as the dispersion relation for the global modes, Eq. (27), under the assumption that $\nu_{sh} \ll \omega$, ω_0 . Another result obtained from the solution to the eigenvalue problem for k_z is that from Eqs. (31) and (32), we have that $\phi_b \gg \phi_0$, which means that the potential and density perturbations are mainly boundary modes that depend on the azimuthal coordinate, a characteristic similar to that of the global modes.

Now, we will try to estimate the magnitude of the axial current produced by these fluctuations using the quasilinear estimates. The perturbations of the azimuthal electric field produce the axial drift velocity

$$\tilde{v}_{ex} = \frac{\tilde{E}_y}{B_0}. \quad (40)$$

This perturbed electron drift results in the axial electron current, whose time average can be calculated at each point along the channel as

$$\langle \tilde{J}_{ex} \rangle = \frac{1}{2} \text{Re}(e \tilde{n}_e \tilde{v}_{ex}^*). \quad (41)$$

Using the expression in Eq. (25) for the perturbed plasma density, along with quasineutrality, and with the azimuthal electric field given by the potential perturbations $\tilde{E}_y = -ik_y \phi$, the averaged axial electron current can be calculated as

$$\langle \tilde{J}_{ex} \rangle = \frac{e^2 n_0 k_y^3 c_s^2}{2B_0 T_e} \frac{|\phi|^2}{|\omega|^2 |\omega + i\nu_{sh}|^2} \omega_r (2\gamma + \nu_{sh}). \quad (42)$$

This estimate can be written in the form

$$\langle \tilde{J}_{ex} \rangle \simeq \frac{n_0 T_e k_y^3 c_s^2}{B_0} \frac{e^2 |\phi|^2}{T_e^2 |\omega|^2}, \quad (43)$$

assuming $|\omega| \simeq \omega_r \simeq \gamma$. For (purely) sound waves with $\omega \simeq k_y c_s$, and $e|\phi|/T_e \simeq 1$, this estimate would lead to the Bohm like current $\langle \tilde{J}_{ex} \rangle \simeq n_0 T_e k_y / B_0$, $k_y = m/r$, where m is the azimuthal wave number and r is the radius. Note that potential fluctuations of the order of $|\phi| = 10$ V were observed in experiments^{13,34} for the exit region.

However, for the boundary modes considered here, Eq. (43) predicts a much lower amplitude for the axial current because the amplitude of density fluctuations proportional to the ratio $k_y^2 c_s^2 / \omega^2$ (see Eq. (25)) is small for the modes under consideration. The suppression of the amplitude of the density response (with respect to the amplitude of potential fluctuations) occurs as a result of the current constraint at the sheath, Eqs. (23) and (24). It is important to note that the sheath response depends on the dielectric constant of the wall material. In the limit $K \gg 1$ (high ϵ and k_y) both the mode frequency and growth rate decrease.¹⁸ In this regime, using the frequency given by Eq. (29), the axial current estimate in Eq. (43) takes the form

$$\langle \tilde{J}_{ex} \rangle \simeq \frac{n_0 T_e}{B_0} k_y \left(\frac{\nu_{sh}}{|\omega_0|} \right)^2 \left(\frac{e|\phi|}{T_e} \right)^2. \quad (44)$$

In the $K \gg 1$ regime, as seen from Eq. (44), the current density does not depend explicitly on either k_y or ϵ . Numerically, for the thruster parameters used above, and $|\phi| \simeq 10$ V, the axial current, calculated from Eq. (44), has a maximum value of the order of 10^2 A/m², consistent with typical experimentally observed values. The current amplitude decreases with increasing magnetic field (downstream towards the exit). The current decrease with magnetic field is weaker than B_0^{-1} ; note that in the $\epsilon \rightarrow \infty$ limit, the magnetic field dependence formally disappears in Eq. (44). The self-consistent evaluation of the anomalous current requires nonlinear theory to determine the fluctuation amplitude as well as the effective wave number.

V. DISCUSSION AND SUMMARY

The stationary $\mathbf{E}_0 \times \mathbf{B}_0$ flow of magnetized electrons is a powerful source of free energy for instabilities in plasmas with unmagnetized ions. A variety of bulk plasma modes driven unstable due to gradients of magnetic field, plasma density, and collisional and ionization effects;^{4,6,7,9–12,35} were considered as potential sources of turbulent transport. In this paper, we considered a new mechanism due to positive feedback between the plasma current into the sheath and the plasma potential fluctuations. This feedback coupling was described as a complex sheath impedance, resulting in the instability of bulk plasma and sheath fluctuations. This shows the dependence of the instabilities on the dielectric properties of the wall material, as was noted earlier from experimental results.¹⁶

The instabilities discussed in the present paper are mainly localized in the region around the peak value of the magnetic field. They have a real part of the frequency in the 1–10 MHz range, giving the azimuthal phase velocity of the order of 6.52×10^5 – 8.03×10^5 m/s for the lowest azimuthal wavenumber $m = 1$. This phase velocity is lower but of the same order of magnitude as the equilibrium $E_0 \times B_0$ electron drift velocity. Similar propagation characteristics have been observed experimentally by Litvak *et al.*²⁹ and Lazurenko *et al.*¹³ for different types Hall thrusters.

The real part of the frequency of both the global and local modes in Eqs. (27)–(37) decreases with increasing

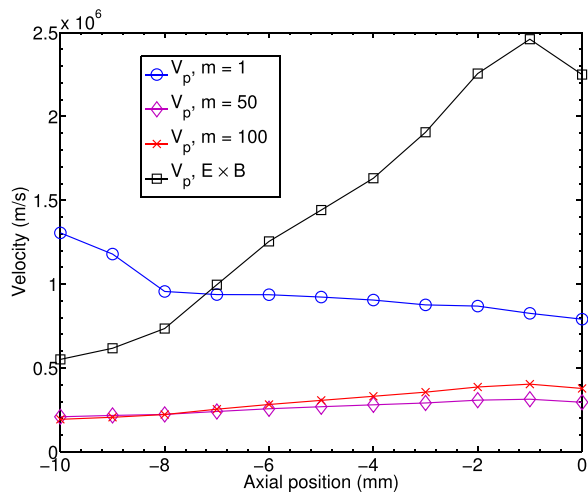


FIG. 6. Azimuthal phase velocities of the instabilities in a SPT-100 thruster³⁰ as a function of axial position from the channel exit as predicted by Eqs. (27) and (37) for different mode numbers and the equilibrium $E_0 \times B_0$ electron drift velocity, $k_y = m/r$, $r = 5$ cm. The exit plane is at $x = 0$.

magnetic field and increases with increasing electric field similar to the behavior observed in experiments performed by Litvak *et al.* and Lazurenko *et al.*, as can be seen in Fig. 4. This is also consistent with the observation that the maximum values of both the real part of the frequency and the growth rate correspond to the region of the maximum equilibrium $E_0 \times B_0$ velocity.

The characteristic phase velocity of the modes studied in our work is weakly sensitive to the mode number, as shown in Figs. 3 and 6. For higher mode numbers, the mode frequency increases, while the phase velocity decreases (see Figs. 3 and 6). In these regimes, kinetic electron cyclotron effects need to be included, but these considerations are outside the scope of our paper. Tsikata *et al.* have observed fluctuations in the 5 kW PPS-X000ML Hall thruster that are located outside of the peak of the magnetic field and have a real part of the frequency of around 4.5 MHz and wavelengths of the order of the electron cyclotron radius.^{14,15} These instabilities are characterized by a phase velocity much smaller than the $E_0 \times B_0$ equilibrium drift velocity and originate due to the resonance of the electron cyclotron frequency with the azimuthal electron drift frequency $k_y v_0$.^{7,14,15}

In our model, wall material effects manifest themselves via the dielectric permittivity of the wall. The walls of the Hall thrusters studied are made of Boron Nitrate (1 kW PPPL Laboratory Hall Thruster) and Borosil, $BNSiO_3$, (SPT-100), whose permittivity can increase with temperature. The thruster walls can reach temperatures of the order of 500 °C, which may result in a permittivity as high as 50. In the present paper, we have considered purely dielectric wall materials (real ϵ). The more general case of finite conductivity (complex permittivity ϵ) is not studied here, though the case with ideally conducting walls can be reproduced in the limit $\epsilon \rightarrow \infty$. Our results indicate that the dielectric permittivity of the wall material acts as an additional parameter that may affect the electron transport and thruster performance and thus its effects are complementary to the secondary electron emission (SEE) effects which are also important for the

electron transport.¹⁶ It is interesting to note that the possible influence of the dielectric properties of the wall material on the thruster performance was noted in Ref. 36.

In this paper, the effect of the dielectric properties of the wall material was considered using the example of ion sound waves. The frequencies of the sheath impedance modes obtained in this paper are in the 2.0–10 MHz range comparable to the typical lower hybrid frequency. A more accurate model that takes into account the electron inertia, which was ignored in the present work, is required but is left for future work. A complete quantitative theory requires also a number of other effects, e.g., plasma gradients, collisions and finite Larmor radius, that are neglected here but that have been considered earlier for the problem of anomalous transport in Hall thrusters.^{6,7,9,11,12}

ACKNOWLEDGMENTS

The authors want to thank the referees for the helpful suggestions for improving this paper. This work was supported in part by NSERC Canada and by the Air Force Office of Scientific Research and the US Department of Energy under Contract No. DEAC02-09CH11466.

- ¹E. Y. Choueiri, *Phys. Plasmas* **8**, 1411 (2001).
- ²C. Boniface, L. Garrigues, G. J. M. Hagelaar, J. P. Boeuf, D. Gawron, and S. Mazouffre, *Appl. Phys. Lett.* **89**, 161503 (2006).
- ³M. Keidar and I. Beilis, *IEEE Trans. Plasma Sci.* **34**, 804 (2006).
- ⁴A. Heron and J. C. Adam, *Phys. Plasmas* **20**, 082313 (2013).
- ⁵S. Tsikata, C. Honore, D. Gresillon, A. Heron, N. Lemoine, and J. Cavalier, in *Proceedings of the 33rd International Electric Propulsion Conference, October 6–10* (IEPC, Washington D.C., 2013).
- ⁶Y. V. Esipchuk and G. N. Tilinin, *Sov. Phys. Tech. Phys.* **21**, 417 (1976).
- ⁷A. Ducrocq, J. C. Adam, A. Heron, and G. Laval, *Phys. Plasmas* **13**, 102111 (2006).
- ⁸T. A. van der Straaten and N. F. Cramer, *Phys. Plasmas* **7**, 391 (2000).
- ⁹A. A. Litvak and N. J. Fisch, *Phys. Plasmas* **11**, 1379 (2004).
- ¹⁰A. A. Litvak and N. J. Fisch, *Phys. Plasmas* **8**, 648 (2001).
- ¹¹A. Kapulkin and M. M. Guelman, *IEEE Trans. Plasma Sci.* **36**, 2082 (2008).
- ¹²W. Frias, A. I. Smolyakov, I. D. Kaganovich, and Y. Raitses, *Phys. Plasmas* **19**, 072112 (2012).
- ¹³A. Lazurenko, V. Krasnoselskikh, and A. Bouchoule, *IEEE Trans. Plasma Sci.* **36**, 1977 (2008).
- ¹⁴S. Tsikata, N. Lemoine, V. Pisarev, and D. M. Gresillon, *Phys. Plasmas* **16**, 033506 (2009).
- ¹⁵S. Tsikata, C. Honore, N. Lemoine, and D. M. Gresillon, *Phys. Plasmas* **17**, 112110 (2010).
- ¹⁶Y. Raitses, I. D. Kaganovich, A. Khrabrov, D. Sydorenko, N. J. Fisch, and A. Smolyakov, *IEEE Trans. Plasma Sci.* **39**, 995 (2011).
- ¹⁷A. Morozov and V. Savelyev, "Fundamentals of stationary plasma thruster theory," in *Reviews of Plasma Physics*, edited by B. Kadomtsev and V. Shafranov (Kluwer, New York, 2000), Vol. 21, pp. 203–391.
- ¹⁸A. I. Smolyakov, W. Frias, I. D. Kaganovich, and Y. Raitses, *Phys. Rev. Lett.* **111**, 115002 (2013).
- ¹⁹A. Simon, *Phys. Rev.* **98**, 317 (1955).
- ²⁰A. Fruchtman, *Plasma Sources Sci. Technol.* **18**, 025033 (2009).
- ²¹T. Lafleur and R. W. Boswell, *Phys. Plasmas* **19**, 053505 (2012).
- ²²F. F. Chen, *Phys. Fluids* **22**, 2346 (1979).
- ²³A. Mikhailovski, *Theory of Plasma Instabilities: Instabilities of a Homogeneous Plasma* (Consultants Bureau, 1974), Vol. 1.
- ²⁴C. N. Lashmore-Davies, *J. Plasma Phys.* **71**, 101 (2005).
- ²⁵B. Kadomtsev, in *7th Conference on Phenomena in Ionized Gases* (Consultants Bureau, 1966), Vol. 2, p. 610.
- ²⁶H. L. Berk, D. D. Ryutov, and Y. A. Tsidulko, *Phys. Fluids B-Plasma Phys.* **3**, 1346 (1991).
- ²⁷R. H. Cohen and D. D. Ryutov, *Contrib. Plasma Phys.* **44**, 111 (2004).
- ²⁸D. D. Ryutov and R. H. Cohen, *Contrib. Plasma Phys.* **44**, 168 (2004).

- ²⁹A. A. Litvak, Y. Raitses, and N. J. Fisch, *Phys. Plasmas* **11**, 1701 (2004).
- ³⁰R. Hofer, I. Mikellides, I. Katz, and D. Goebel, in *43rd AIAA/ASME/SAE/ASEE Joint Propulsion Conference & Exhibit*, AIAA 2007 (2007).
- ³¹Y. Raitses, M. Keidar, D. Staack, and N. Fisch, *J. Appl. Phys.* **92**, 4906 (2002).
- ³²F. Parra, E. Ahedo, J. Fife, and M. Martinez-Sanchez, *J. Appl. Phys.* **100**, 023304 (2006).
- ³³J. Fife, "Aeronautics and Astronautics," Ph.D. thesis (Massachusetts Institute of Technology, 1998).
- ³⁴A. W. Smith and M. A. Cappelli, *Phys. Plasmas* **16**, 073504 (2009).
- ³⁵E. Fernandez, M. K. Scharfe, C. A. Thomas, N. Gascon, and M. A. Cappelli, *Phys. Plasmas* **15**, 012102 (2008).
- ³⁶E. Raitses, J. Ashkenazy, G. Appelbaum, and M. Guelman, in *International Electric Propulsion Conference*, IEPC-1997 (1997).